16-Channel Optical Add-Drop Multiplexer Consisting of a Planar Waveguide Concave Grating

CHUN-TING LIN
National Chiao Tung University
Department of Photonics and
Institute of Electro-Optical Engineering
1001 Ta-Hsueh Road, Hsinchu
Taiwan

YANG-TUNG HUANG
National Chiao Tung University
Department of Electronics Engineering
and Institute of Electronic
1001 Ta-Hsueh Road, Hsinchu
Taiwan

JUNG-YAW HUANG
National Chiao Tung University
Department of Photonics and
Institute of Electro-Optical Engineering
1001 Ta-Hsueh Road, Hsinchu
Taiwan

Abstract: A new 16-channel optical add-drop multiplexer (OADM), which consists of one planar waveguide concave grating, two main ports, coupled waveguides, sixteen add ports, sixteen drop ports, and sixteen sets of 2×2 switches, is proposed. The transmission characteristics of the light detected at the output waveguide are simulated by using a design example. The on-off crosstalks are less than -35.17 dB with the insertion losses of 4.71 to 4.83 dB.

Key–Words: Planar waveguide, Integrated optics, Concave grating, Optical add-drop multiplexer, Wavelength-division multiplexing

1 Introduction

Wavelength division multiplexing systems use each wavelength signal as a separate channel. Wavelength signals can be coupled into and dropped out of the fiber by a multiplexer and a demultiplexer. The functions of an optical add-drop multiplexer (OADM) is to transmit and drop the wavelength signals selectively. In a conventional design, an OADM consists of arrayed-waveguide gratings (AWGs) [1, 2]. However, AWGs encounter the inherent limits due to the larger die size and the lower free spectral range [3]. In this paper, a new OADM consisting of a planar waveguide concave grating is proposed to remedy these disadvantages of AWGs.

The schematic configuration of the 16-channel OADM is shown in Fig. 1. It consists of one planar waveguide concave grating, two main ports, coupled waveguides, sixteen add ports, sixteen drop ports, and sixteen sets of 2×2 switches. 16 wavelength signals, λ_1, λ_2,...λ_{16}, transmitted by the main port (left-side) are demultiplexed by the concave grating and then coupled into the 2×2 switches while 16 waveguide signals, λ_1', λ_2',...λ_{16}', with the same channel spacing are coupled into the corresponding add ports at the same time. After transmitting and dropping the signals selectively by the 2×2 switches, the signals are multiplexed by the concave grating and then coupled into the main port (right-side) again. In this paper, a concave grating with specifically designed tilt angles of both sides for each grating facet is proposed.

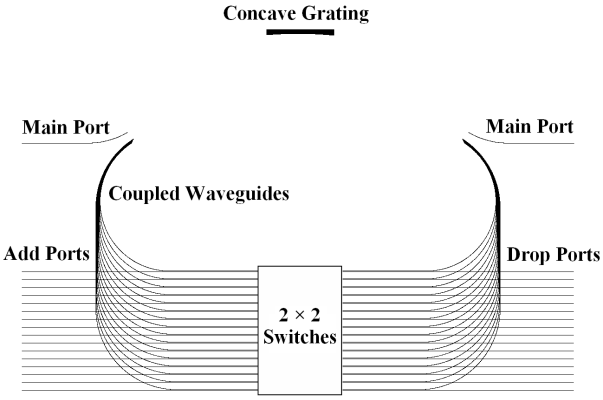

Figure 1: Schematic configuration of the 16-channel optical add-drop multiplexer system.

2 Design Formula

If the input waveguide (left-side main port) and the coupled waveguide (left-side) are located at (a_1, b_1) and (a_2, b_2) as shown in Fig. 2, the output waveguide (right-side main port) and the coupled waveguide (right-side) are located at ($-a_1$, b_1) and ($-a_2$, b_2), respectively. Using the recursive-definition method [4, 5], the free-aberration position of each groove is determined from the solution for the root of the following function:

$$F(x_i, y_i) = r_{1,i} + r_{2,i} + im\lambda_0/n_{\text{eff}} - r_{1,0} - r_{2,0} = 0, \quad (1)$$

where $(x_i,\ y_i)$ denotes the position of the vertex for the ith groove, $r_{j,i}$ denotes the distance between $(a_j,\ b_j)$ and $(x_i,\ y_i)$, m denotes the diffraction order, λ_0 denotes the design wavelength, and n_{eff} denotes the effective index in the slab waveguide. The optimum tilt angle θ_i of the ith grating facet with respect to the x-axis can be obtained as [4]

$$\theta_i = \tan^{-1}\left(-\frac{\frac{a_1-x_i}{r_{1,i}}+\frac{a_2-x_i}{r_{2,i}}}{\frac{b_1-y_i}{r_{1,i}}+\frac{b_2-y_i}{r_{2,i}}}\right). \quad (2)$$

The optimum tilt angle φ_i of the other side for the ith grating facet with respect to the x-axis can be obtained as

$$\varphi_i = \tan^{-1}\left(-\frac{\frac{-a_1-x_i}{r_{1,i}}+\frac{-a_2-x_i}{r_{2,i}}}{\frac{b_1-y_i}{r_{1,i}}+\frac{b_2-y_i}{r_{2,i}}}\right). \quad (3)$$

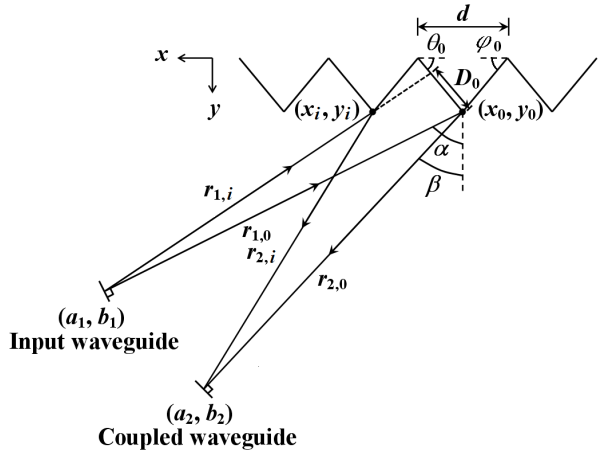

Figure 2: Schematic figure of the light diffracted by the concave grating.

In our simulation, a Gaussian field model [6] launched from the input waveguide is diffracted by the concave grating, refocused at the imaging curve, and guided into different coupled waveguides according to the corresponding wavelengths. After transmitting and dropping wavelength signals selectively by the 2 $\times$ 2 switches, the reverse function takes place by the same grating. The imaging equation for the concave grating has the following form:

$$\frac{\cos\alpha}{R}-\frac{\cos^2\alpha}{r_{1,0}}+\frac{\cos\beta(f)}{R}-\frac{\cos^2\beta(f)}{r_{2,0}(f)}=0, \quad (4)$$

where α and β denote the incident angle and the diffraction angle of the input Gaussian beam at the grating pole, respectively, and R is the effective radius of the grating.

The spectral response of each coupled waveguide can be obtained from the following overlap integral of the imaging field E_1 with mode field E_2 of the coupled waveguide:

$$I(f)=\frac{\left|\int E_1(f,x'')\cdot E_2^*(f,x'')dx''\right|^2}{\int|E_1(f_0,x'')|^2\,dx''\cdot\int|E_2(f_0,x'')|^2\,dx''}\cdot\Gamma, \quad (5)$$

where Γ denotes the loss attributed to the grating or the waveguide including the undesired-order loss and the propagation loss. When all 2 $\times$ 2 switches are off, the transmission characteristic $T(f)$ of the light detected at the main port (right-side) in Fig. 1 can be obtained as

$$T(f)=\sum_j I_j(f)\cdot I_j'(f) \quad (6)$$

where $I_j(f)$ denotes the spectral response for the main port (left-side) incidence to the jth coupled waveguide (left-side) and $I_j'(f)$ denotes the spectral response for the main port (right-side) incidence to the jth coupled waveguide (right-side). When the selected jth switch is turned on, the selected jth signal is extracted from the main port to the drop port [2]. And $I_j(f)$ in (6) will be exchanged with the spectral response $I_{\text{add},j}(f)$of the jth add port.

3 Design Example

For a design example, the waveguide consists of a 6-μm-thick SiON core layer with an upper 6-μm-thick and a lower 10-μm-thick SiO_2 cladding layers. The side views of the channel waveguide and the slab waveguide is shown in Fig. 3. The grating can be achieved by etching a trench to the lower cladding layer and then coated with metal at the back wall. The refractive indices of SiO_2 and SiON are 1.450 and 1.456, respectively, and the refractive index of the silicon substrate is 3.476 at a design wavelength of 1550.12 nm. Using the transfer matrix method [7], the effective indices of TE and TM modes are 1.45393 and 1.45392 with the propagation losses, obtained from the imaginary parts of the effective indices, of 4.90 $\times$ 10^{-3} dB/cm and 2.75 $\times$ 10^{-2} dB/cm, respectively.

There are 16 channels in the C-band with a channel spacing of 0.4 nm (50 GHz) according to ITU grids [8]. We take the TE mode for example so the effective index of the slab waveguide is 1.45393 at a design wavelength of 1550.12 nm. The grating period is $d = 10$ μm operating at the diffraction order $m = 16$ with a free spectral range of 96.88 nm. α = 60° is the incident angle for the main port (left-side) with a diffraction angle β = 57.12°. The distance from the end of the input waveguide (left-side main port) to the grating pole is $r_{1,0}$ = 25000 μm and the distance from

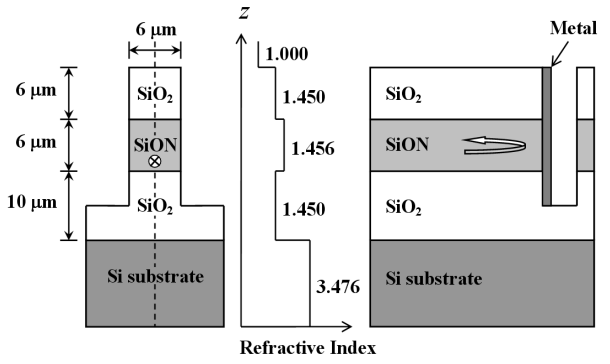

Figure 3: Side views of the channel waveguide (left) and the slab waveguide (right).

the coupled waveguide (left-side) of the central channel to the grating pole is $r_{2,0}$ = 25000 μm as shown in Fig. 2. The grating is designed for the main port (left-side) incidence to the coupled waveguide (left-side) of the central channel. $\alpha' = -60^\circ$ is the incident angle for the main port (left-side) with a diffraction angle $\beta' = -57.12^\circ$. The distance from the output waveguide (right-side main port) to the grating pole is $r'_{1,0}$ = 25000 μm and the distance from the coupled waveguide (right-side) of the central channel to the grating pole is $r'_{2,0}$ = 25000 μm. The total number of grating periods is calculated to be 885 with an effective radius of the grating R = 47754 μm from (4). The total device size is 70 $\times$ 46 mm^2 with a separation between two neighbor coupled waveguides of 1000 μm.

Assuming no scattering loss and side-wall tilt loss at the grating facet, the spectral responses I_j of 16 channels for the main port (left-side) incidence to the corresponding coupled waveguides (left-side) are shown in Fig. 4. The insertion loss of the central channel is 2.37 dB, which includes the excess loss, the coupling loss from the slab waveguide to the output channel waveguide, and the undesired-order loss, the loss for the diffraction of the light into undesired adjacent orders. The propagation loss is negligible in our case. The spectral responses I'_j for the main port (right-side) incidence to the coupled waveguides (right-side) are shown in Fig. 5. The insertion loss of the central channel is 2.40 dB.

When the switches SW_2, SW_5, SW_6, SW_8, SW_9, SW_{12}, SW_{15}, and SW_{16}, for example, are turned on, the selected signals are extracted from the main port to the drop port and the transmission characteristic $T(f)$ in (6) is shown in Fig. 6. Here, the signals from the add port are not considered and the background noise is set to be lower than -40 dB. The insertion losses and the on-off crosstalks caused by the switches are not considered. It shows that the on-off crosstalks are less than -35.17 dB with the insertion losses of 4.71 to 4.83 dB. The proposed scheme is feasible for the design of an OADM due to the smaller die size of 70 $\times$ 46 mm^2, the higher free spectral range of 96.88 nm, and the higher spectral resolution for the channel spacing of 0.4 nm (50 GHz) compared with [2].

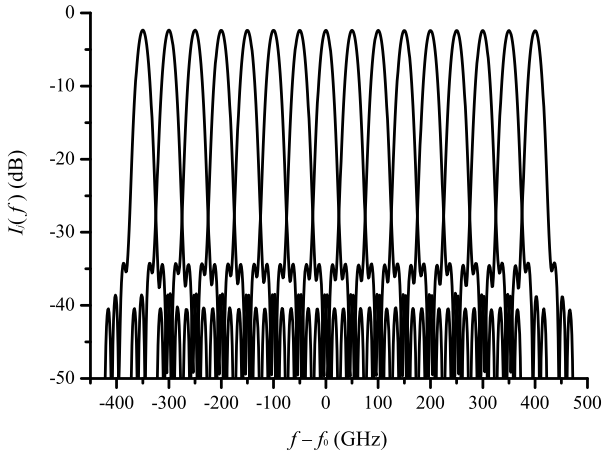

Figure 4: 16-channel spectral responses $I(f)$ for the main port (left-side) incidence to the coupled waveguides (left-side).

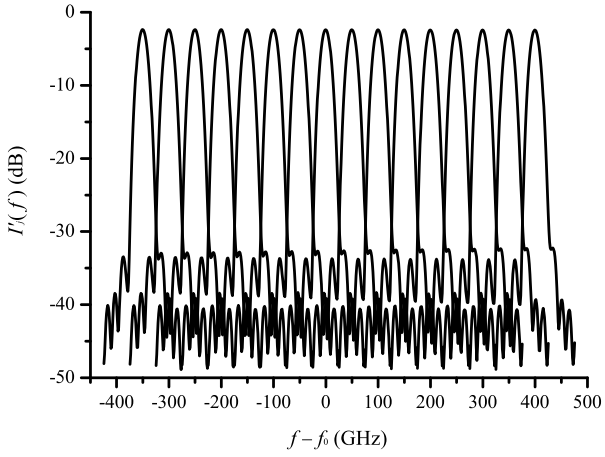

Figure 5: 16-channel spectral responses $I'(f)$ for the main port (right-side) incidence to the coupled waveguides (right-side).

4 Conclusion

In this paper, an optical add-drop multiplexer consisting a planar waveguide concave grating is proposed. The transmission characteristics $T(f)$ is simulated with a design example. The on-off crosstalks are less than -35.17 dB with the insertion losses of 4.71 to 4.83 dB. Simulation results show that the proposed scheme is feasible for the design of an OADM

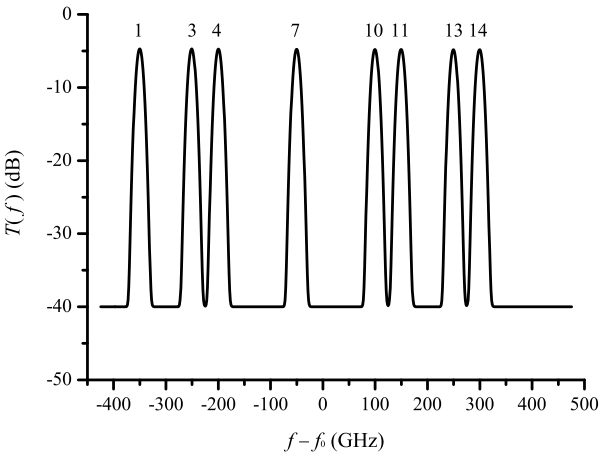

Figure 6: Transmission characteristics $T(f)$ detected at the main port (right-side).

and will be widely used in all-optical WDM systems due to its good performance.

Acknowledgements: The research was supported by the National Science Council of the Republic of China under Contract NSC96-2221-E-009-111.

References:

[1] K. Okamoto, K. Takiguchi, and Y. Ohmori, 16-channel optical add/drop multiplexer using silica-based arrayed-waveguide gratings, *Electron. Lett.* 31, 1995, pp. 723–724.

[2] K. Okamoto, M. Okuno, A. Himeno, and Y. Ohmori, 16-channel optical add/drop multiplexer consisting of arrayed-waveguide gratings and double-gate switches, *Electron. Lett.* 32, 1996, pp. 1471–1472.

[3] S. Janz, A. Balakrishnan, S. Charbonneau, P. Cheben, M. Cloutier, A. Delâge, K. Dossou, L. Erickson, M. Gao, P. A. Krug, B. Lamontagne, M. Packirisamy, M. Pearson, and D.-X. Xu, Planar waveguide echelle gratings in silica-on-silicon, *IEEE Photon. Technol. Lett.* 16, 2004, pp. 503–505.

[4] K. A. McGreer, Theory of concave gratings based on a recursive definition of facet positions, *Appl. Opt.* 35, 1996, pp. 5904–5910.

[5] C.-T. Lin, Y.-T. Huang, J.-Y. Huang, and H.-H. Lin, Integrated planar waveguide concave gratings for high density WDM systems, *2005 Optical Communications Systems and Networks*, IASTED, Canada 2005, pp. 98–102.

[6] K. A. McGreer, Diffraction from concave gratings in planar waveguides , *IEEE Photon. Technol. Lett.* 7, 1995, pp. 324–326.

[7] T. Tamir, Ed., *Guided-Wave Optoelectronics*, Springer–Verlag, Berlin–Heidelberg–New York–London–Paris–Tokyo 1990, pp. 43–50.

[8] S. V. Kartalopoulos, *Introduction to DWDM Technology*, IEEE-Press, New York 2000, pp. 184.